Surface Properties of Block and Graft Polystyrene–Polydimethylsiloxane Copolymers

Ningjing Wu,[1] Likan Huang,[1] Anna Zheng,[1] Huining Xiao[2]

[1]*Key Laboratory for Ultrafine Materials, Ministry of Education, East China University of Science and Technology, Shanghai 200237, People's Republic of China*
[2]*Department of Chemical Engineering, University of New Brunswick, Fredericton, New Brunswick, Canada E3B 5A3*

Received 11 November 2004; accepted 3 May 2005
DOI 10.1002/app.22978
Published online 11 January 2006 in Wiley InterScience (www.interscience.wiley.com).

ABSTRACT: The surface compositions of a series of polystyrene-*b*-polydimethylsiloxane (PS-*b*-PDMS) and polystyrene-*g*-polydimethylsiloxane (PS-*g*-PDMS) copolymers were investigated using ATR-FTIR and XPS technique. The results showed that enrichment of PDMS soft segments occurred on the surface of the block copolymers as well as on that of graft copolymers. And the magnitude order of the enrichment was as follows: PS-*b*-PDMS > PS-*g*-PDMS, which was attributed to the facilitating of the movement of the PDMS segments in PS-*b*-PDMS copolymer. Meanwhile, the solvent type and the contact medium had influence on the accumulation of PDMS on the surfaces. © 2006 Wiley Periodicals, Inc. J Appl Polym Sci 99: 2936–2942, 2006

Key words: block copolymer; graft copolymer; surface property

INTRODUCTION

Much attention has been recently paid to the analysis of polymer surfaces and to the tailored modification of their properties. In fact, a variety of applications are directly related to the surface characteristics of polymeric materials, such as friction, permeability, adhesion, and biocompatibility.

The block or graft copolymers, which are comprised of covalent-bonded incompatible polymer segments, generally result in microphase separation structure, and their surfaces tend to be covered with one component with the lower surface energy over the sublayer of another component with the higher surface energy. The low surface tension part of such copolymers is responsible for the surface accumulation of the copolymer, whereas the matrix compatible component acts as an anchoring block and ensures the permanency of the surface modification. This anchoring effect accounts for the superiority of these copolymers over low-molecular-weight surfactants, which are easily migrated, excluded, or washed out from the surface.[1–5]

Preliminary papers have focused on the surface activity of poly(styrene-*b*-dimethylsiloxane) (PS-*b*-PDMS) and different copolymers containing polydimethylsiloxane (PDMS).[6–12] The surface segregation of PDMS of copolymer films in AB diblock and ABA and BAB triblock types has been investigated with the electron spectroscopy for chemical analysis (ESCA) or X-ray photoelectron spectroscopy (XPS)[13–15] and attenuated total reflectance (ATR-FTIR).[1] However, systematic studies on the effects of cast substrate and cast solvents on surface morphology and composition of copolymers have been seldom reported.

The main objective of this work was to perform a systematic investigation on the PDMS accumulation of on the surface and near surface regions in both PS-*b*-PDMS and PS-*g*-PDMS copolymers, based on the measurements of ATR-FTIR, contact angles, and XPS. The PS-*b*-PDMS block copolymers were synthesized by a sequential anionic polymerization, whereas the PS-*g*-PDMS graft copolymers were prepared through a macromonomer approach. The impact of contact substrates and the solvent types (i.e., those with different solubility) on the accumulation of PDMS were also investigated.

EXPERIMENTAL

Materials

Styrene (CP. Jinshan Petrochemical Co., Shanghai, China) was washed with dilute sodium hydroxide to remove any inhibitors, dried over calcium hydride, and distilled under reduced pressure just prior to use. Cyclohexane, tetrahydrofuran, and DMF (AR. Shanghai Feida Industry Trade Co., Ltd., Shanghai, China) were refluxed over sodium and distilled just before use. Hexamethylcyclotrisiloxane (D_3) (CP. Huaxin Chemical Co., Xiamen, China) was dried over calcium

Correspondence to: A. Zheng (zan@ecust.edu.cn).

hydride and freshly baked using 4A molecular sieves. *n*-BuLi initiator (1.0*M*) in cyclohexane was made with reference to literature.[16] Azobis(isobutyronitrile) (AR) was purchased from Shanghai Feida Industry, without further purification.

PDMS macromonomer was prepared through anionic polymerization of D_3, with vinylchlorosiloxane as terminator, to afford double functional bond.

The synthesis of PS-*b*-PDMS copolymer

PS-*b*-PDMS copolymer was synthesized by the sequential anionic polymerization of styrene and D_3. Styrene polymerization was first induced with *n*-BuLi initiator in cyclohexane at room temperature. The reaction was carried out for 0.5 h. D_3 and DMF were successively added to living polystyrene (PS) chains as a promoter. Afterward, the polymerization proceeded continuously at 60°C for 6 h. The block copolymer chains were deactivated by methanol and precipitated in methanol, filtered, and dried in vacuum at 80°C for 24 h, followed by removing the homopolymers with solvents. To remove PDMS homopolymer, hexane was used. And to eliminate PS homopolymer, a solvent mixture (cyclohexane:hexane = 25 : 1.2 wt/wt) was used.

The synthesis of PS-*g*-PDMS copolymer

The free-radical copolymerization of the PDMS macromonomer with styrene was performed in bulk at 60°C for 24 h, using 0.1 wt % azobis(isobutyronitrile) as an initiator, under a nitrogen atmosphere. The product was precipitated with ethanol. The homopolymers, PDMS and PS, were removed by a mixed solvent. The graft copolymer was dried under vacuum at 80°C to a constant weight.

Film preparation

Films were prepared by casting 10 wt % solutions of PS-*b*-PDMS or PS-*g*-PDMS in toluene, cyclohexane, or bromobenzene, respectively. Several substrates were selected, including clean glass slides and polytetrafluoroethylene (PTFE) plates. Deposited films were dried under vacuum for 48 h before analysis. Solvent-cast films were carefully peeled from the substrate, allowing the measurements of contact angles and the recording of ATR-FTIR spectra and XPS spectra to be performed, not only at the polymer/air interfaces but also on the substrate sides.

Charaterization of copolymer structures

Contact angles

The contact angles of PS-*g*-PDMS and PS-*g*-PDMS copolymer films were determined using a static drop contact angle/interface tension meter (Model -JC2000A, Zhongchen Digital Ltd., Shanghai). Surface tension was calculated, based on the contact angle of water and diiodomethane droplets on polymer films at 20°C (Table I). The Owens and Wendt's method[6] was adopted, and the formula for calculation is as follows:

TABLE I
Surface Energy of H_2O and CH_2I_2[12]

Liquid	r_s (10^{-3} N/m)	r_s^d (10^{-3} N/m)	r_s^p (10^{-3} N/m)
H_2O	72.8	22.1	50.7
CH_2I_2	50.8	48.5	2.3

$$-r_l \cos\theta = r_l - 2(r_s^d r_l^d)^{1/2} - 2(r_s^p r_l^p)^{1/2}$$

where θ is the contact angle; r_l, r_l^d, r_l^p represent free surface energy, dispersive, and polar interactions of liquids, whereas r_s, r_s^d, r_s^p represents free surface energy, dispersive, and polar interactions of solids or polymer films, respectively.

ATR-FTIR experiments were performed using a Nicolet AVATAR360 FTIR spectrometer equipped with a DTRS detector. To collect ATR-FTIR spectra, 512 scans were run. Being mounted on a Harrick TPMRA attachment, a Harrick parallelogram Ge prism with 45° face cut was used as the internal reflectance element for all ATR-FTIR collections.

The ATR-FTIR spectra of PS and PDMS and PS-*b*-PDMS copolymer are shown in Figure 1. PS has a characteristic absorption peak at 1495 cm^{-1}, while PDMS at same wave numbers has scarcely any characteristic absorption, and PDMS has a very strong absorption peak at 1495 cm^{-1}, while PS has scarcely any characteristic absorption at same wave numbers. So quantitative calculations of the PDMS and PS molar fraction were based on the peak area ratio A_{1261}/A_{1496} obtained ATR-FTIR measurements. After our calibration, the following equation has been well received and also adopted in our calculation.

$$A_{1261}/A_{1495} = 0.520(X/1 - X)$$

where A_{1261} is the area of absorption peak at 1261 cm^{-1} of PDMS, A_{1495} is the area of absorption peak of PS at 1495 cm^{-1}, and X is the PDMS molar fraction.

^{1}H NMR spectroscopy was performed on a 500 MHz AVANCE500 spectrometer, with $CDCl_3$ as the solvent and TMS as the calibration. ^{1}H NMR Spectra of PS-*b*-PDMS coplymers show the characteristic peaks of both segments; for example, ortho protons of the phenyl ring at 6.65, meta and para protons at 7.15 due to a PS segment, and a sharp single at 0.15 due to

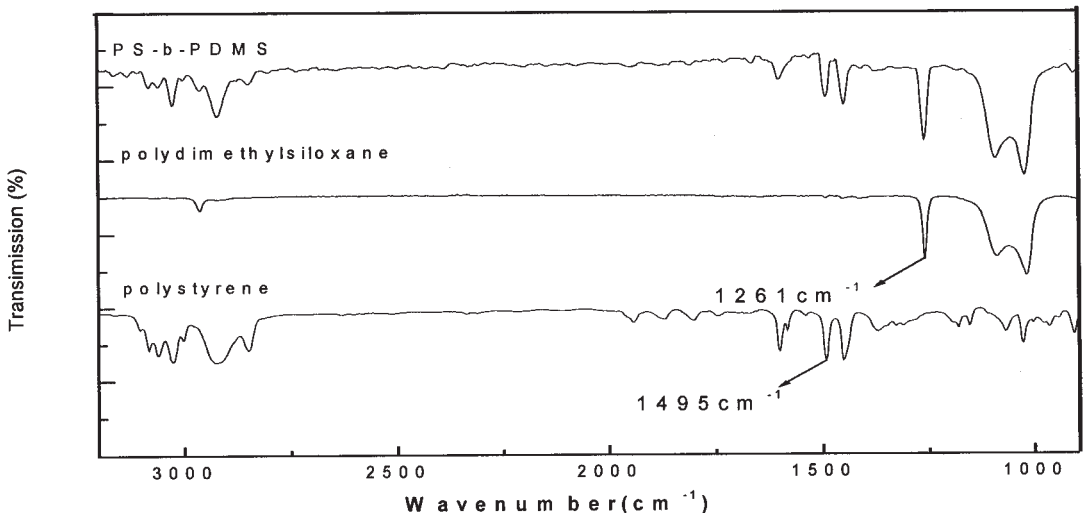

Figure 1 The ATR-FTIR spectra of polymers.

Me_2Si protons of PDMS. The molar fraction of PS-*b*-PDMS or PS-*g*-PDMS copolymer in bulk can be calculated from the proton areas of PS segments and PDMS segments.

XPS

Photoelectron spectra were recorded using a PHI 5000C ESCA spectrometer (Philip Company), to determine surface atomic ratios and the depth distribution of polymers. The instrument was equipped with a monochromatized Al K X-ray source ($h\upsilon$ = 14.0 keV). Depth distribution of the PS-*b*-PDMS and PS-*g*-PDMS from the film surface was analyzed by recording the XPS spectra at various electron erosion times. The quantitative analysis of silicon and oxygen and carbon was performed with the aid of PHI-MATLAB software.

RESULTS AND DISCUSSION

The characterization of PS-*b*-PDMS and PS-*g*-PDMS copolymers

PS-*b*-PDMS copolymers were synthesized by a sequential anionic polymerization, whereas, PS-*g*-PDMS copolymers were prepared using a macromonomer approach, through which a graft copolymer with well-defined structures (i.e., PDMS segment length and graft density) could be produced. Table II shows the PDMS molar fractions and molecular mass of the copolymers measured by GPC; samples 1–3 were AB-type diblock copolymers, and sample 4 was a graft copolymer.

Surface composition of PS-*b*-PDMS and PS-*g*-PDMS copolymer films at different interfaces

The ATR-FTIR spectra of a PS-*b*-PDMS copolymer (PDMS feed fraction: 37.6%) in toluene, at the different interfaces, are shown in Figure 2. Based on A_{1261}/A_{1496} peak ratios, PDMS fractions at various interfaces can be estimated, as addressed previously. The film was sliced in parallel with the surface for the bulk ATR-FTIR measurement. The results are presented in the second row in Table III. Similar ATR-FTIR measurements were performed for the other three copolymers, and the results are also presented in Table III. It should be noted that the bulk PDMS fraction was measured by ^{1}H NMR. The results in Table III suggested that PDMS fractions, obtained from ATR-FTIR measurements, were higher at the air surface than those in bulk, both for AB diblock and graft copolymers. Moreover, the lower the bulk PDMS fraction, the higher the PDMS enriched at interfaces. For example, when the bulk PDMS fraction was 0.199, the corresponding fraction at the air surface was 0.736–3.7 times as much as that in the bulk. When the bulk PDMS fraction was 0.376, the PDMS fraction at the air surface was 0.775, only twice as much as that in the bulk. Surprisingly, a similar behavior was observed on the glass slide, which has a higher surface energy than that of copolymer matrix. However, the ATR-FTIR measurement still showed that the PDMS enrichment at the glass interface was lower than that at the air interface.

TABLE II
The Characterization Data for PS-*b*-PDMS and PS-*g*-PDMS Copolymers by GPC

Sample	Type	PDMS content (molar fraction)	M_n (10^{-3})		
			Copolymer	PS block	PDMS block
1	PS-*b*-PDMS	0.448	146.2	80.7	65.5
2	PS-*b*-PDMS	0.376	90.3	56.3	34.0
3	PS-*b*-RDMS	0.199	88.2	70.6	17.6
4	PS-*g*-PDMS	0.199	86.1	69.0	17.1

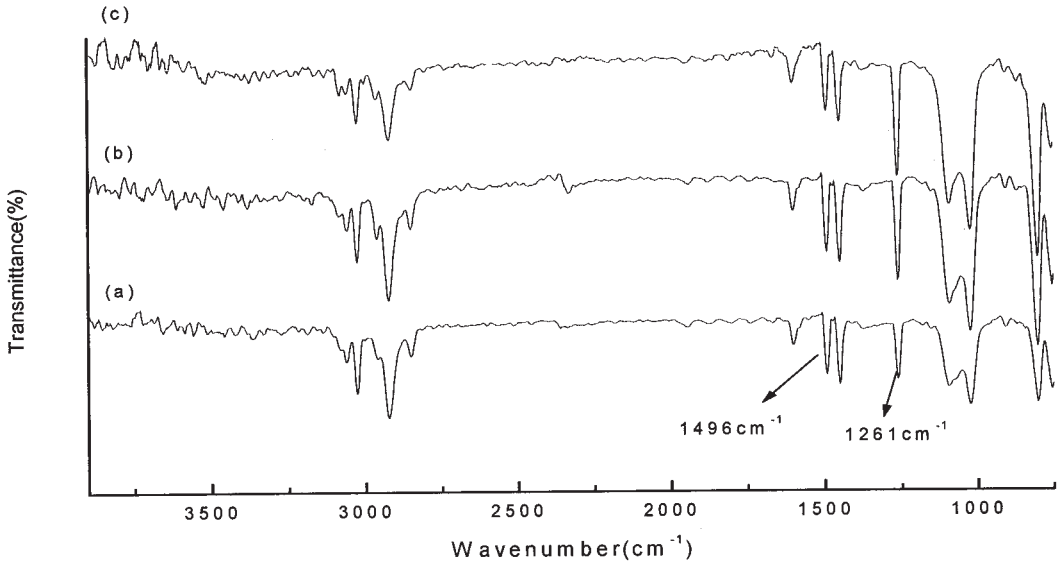

Figure 2 ATR-FTIR spectra of PS-*b*-PDMS at different interfaces ($X_{PDMS} = 0.376$).

A PDMS segment has a very low surface energy (20.4 mN/m at 20°C). In contrast, a PS segment has a much higher surface energy (40.7 mN/m at 20°C). Such a difference in surface energy as well as the high mixing enthalpy for the two different segments in the PS-PDMS copolymers drives the PDMS segment to segregate to the free surface. This is a thermodynamic-favor process, minimizing the total free energy of the copolymer systems.

The PDMS segment migrates to the interface selectively, and tends to accumulate at the air interface or the substrate interface, with a low surface energy. Because PTFE has a low surface energy, the PDMS segments are readily accumulated at the PTFE interface, leading to a higher PDMS fraction at the PTFE interface than that at the glass interface. Overall, the contact substrate indeed affects the accumulation of PDMS at the interface. It is an advantage for the PDMS segment to migrate at the substrate of lower energy.

The effect of the architecture of copolymers on PDMS surface segregation can also be seen from the results in Tables II and III. The PDMS chain length and the number-avearge molecular weight of copolymer sample 4 were close to those of copolymer sample 3. Two samples had comparable bulk PDMS fractions. However, sample 4 had a lower PDMS surface concentration. This is attributed to the fact that the PDMS segments in the block architecture had one free end and another end connected to PS segments. The free ends of the PDMS blocks facilitated the migration of PDMS segment to the surface region, while the situation for PS-*g*-PDMS copolymer with several PDMS as branched segments was different. Although the branched PDMS segments were still relatively free, having the PS backbone constraint applied on them, the PDMS segments could not migrate as freely as the one in diblock polymer. As a result, the surface concentration in PS-*g*-PDMS copolymer was substantially lower than that in PS-*b*-PDMS copolymer.

TABLE III
The Composition of PS-*b*-PDMS and PS-*g*-PDMS Copolymers at Different Interfaces

	Content of PDMS segment (molar fraction)			
Sample	Bulk	Air surface	Glass interface	PTFE interface
PS-*b*-PDMS	0.448	0.974	0.856	0.958
PS-*b*-PDMS	0.376	0.775	0.703	0.764
PS-*b*-PDMS	0.199	0.736	0.498	0.672
PS-*g*-PDMS	0.199	0.537	0.458	0.497

Surface composition of PS-PDMS copolymer films cast from different solvents

Films were prepared by casting solutions of PS-*b*-PDMS copolymer in toluene, cyclohexane, and bromobenzene, respectively. The ATR-FTIR spectra of PS-*b*-PDMS copolymer films cast from different solvents at air interface were shown in Figure 3, and the results on molar fractions are presented in Table IV. As can be seen from the table, the compositions of the films at air interface varied, as different solvents were used, in spite of the same bulk concentration being maintained. The PDMS concentration cast from bromobenzene was relatively lower than those cast from toluene and cyclohexane.

When the PS-*b*-PDMS copolymer was cast from toluene at a low polymer concentration, both PDMS and PS components in the block copolymer were well sol-

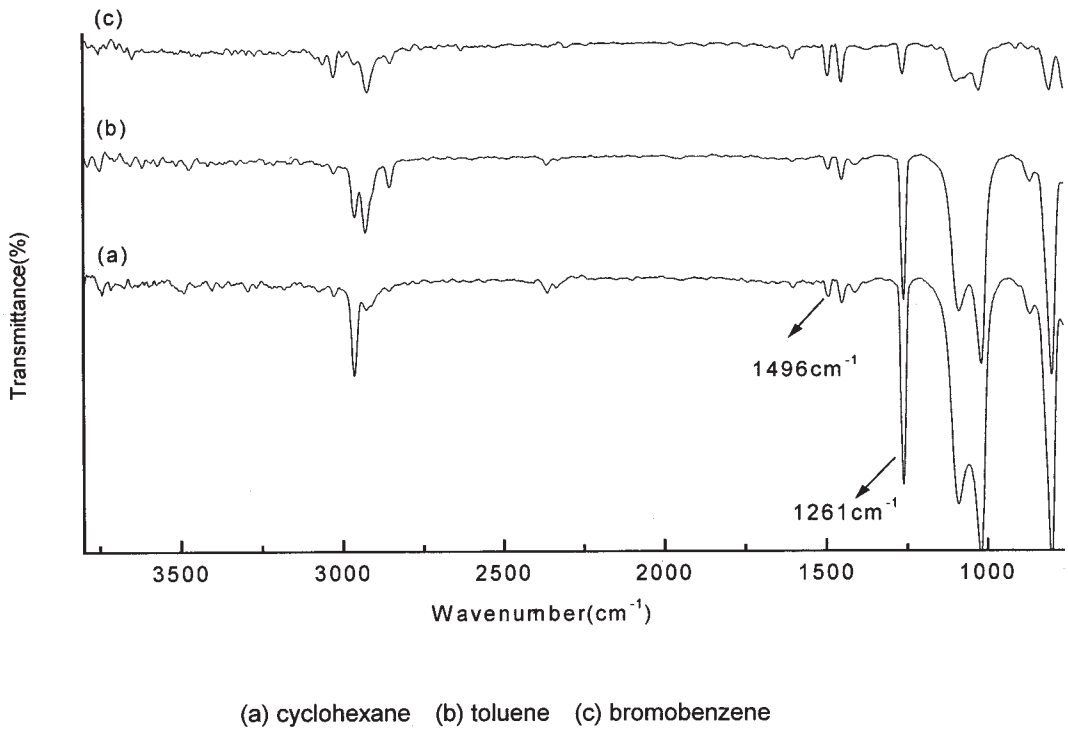

Figure 3 ATR-FTIR spectra of PS-*b*-PDMS films cast from the different solvents at air interface.

ubilized in the solution, as toluene was a good solvent for both. According to the relationship between the polymer–solvent interaction parameters and the polymer concentration, the solubility parameter of PS block was close to that of toluene, the PS blocks in the block copolymers became more soluble, as the polymer concentration increased. Meanwhile, the PDMS blocks in the block copolymers became less soluble, and so toluene preferentially solubilized the PS blocks of the PS-PDMS block copolymers in high polymer concentrations. As a result of the difference in solubility, PDMS blocks separated from the PS blocks and spontaneously accumulated themselves at the air surface. When PS-*b*-PDMS copolymer film was cast from cyclohexane, which was a preferential solvent for PDMS, the PDMS blocks in the copolymers became more soluble than PS blocks, and the PDMS segment conformation was completely extended, while the PS segment conformation was coiled in the solution. Consequently, the PDMS segment was easier to migrate to the interface cast from the cyclohexane than from toluene. Similarly, bromobenzene was a good solvent for PS blocks, and the PDMS segment conformation was coiled while the PS segment was totally extended in the copolymer solution, and so the PDMS blocks were less easier to migrate to the interface. Overall, the order of degree of PDMS enrichment at the interface was as follows: cyclohexane > toluene > bromobenzene.

The depth profile of PS-*b*-PDMS and PS-*g*-PDMS was analyzed on the copolymer films using XPS. The profiles of PDMS molar fraction versus sampling depth for the PS-PDMS copolymers films, cast from toluene, are shown in Table V. XPS provided the con-

TABLE IV
The Surface Composition of PS-*b*-PDMS in Different Solvents at Air Interface in Sample 1

Solvent	δ^a $(10^{-3}$ J/m$^3)^{1/2}$	PDMS segment content (molar fraction)	
		Bulk	Air surface
cyclohexane	14.9	0.484	0.998
toluene	18.2	0.484	0.974
bromobenzene	19.4	0.484	0.489

δ, solubility parameter; δ_{PDMS} = 15.l; δ_{PS}.= 18.6.[17]

TABLE V
Surface Composition of PDMS of PS-PDMS Copolymers

Sample	Erosion depth (Å)	PDMS content (molar fraction)		PS content of air surface
		Bulk	Air surface	
PS-*b*-PDMS	15	0.199	0.813	0.187
	35		0.809	0.191
	55		0.793	0.207
PS-*g*-PDMS	15	0.199	0.647	0.353
	35		0.648	0.352
	55		0.623	0.377

centration gradient of PDMS at the air surface from 15 to 55 Å in depth, revealing the distribution profile of the PDMS.

Evidently, the PDMS segments of PS-PDMS copolymer films cast from toluene accumulated at the surface and subsurface. At the similar bulk composition, the PDMS segments in the PS-*b*-PDMS diblock copolymer were more prone to segregating in the free surface region, whereas the PDMS segments in the PS-*g*-PDMS copolymer were less prone to migrating to the free surface region. These findings were consistent with the results addressed previously. The profile distribution also indicated that a small amount of PS was detected at the air interface, along with the PDMS components. The surface morphologies of the PS-PDMS copolymers appeared to be lamellar if the PDMS molar fraction in the bulk was high (>0.6). The outermost surface region of copolymers was composed of the nearly pure PDMS component.[3] For the copolymers with a low PDMS molar fraction in the bulk (<0.5), the segregation of PDMS in the same surface region was still high. However, a substantial amount of the PS component was also present in this layer, so that the surface morphologies of the copolymer tended to be spherical, where the PDMS segments were of continuous phase, while PS was of dispersed phase.

In a wider surface region, there existed either PDMS segments or both PDMS and PS segments, depending on the segment architecture, bulk fraction, and surface morphology. Among these three features, the segment architecture and surface morphology had more profound effects on the surface compositions of the copolymers. PS-*b*-PDMS diblock copolymers tended to have higher surface segregation of the PDMS blocks than PS-*g*-PDMS graft copolymers at similar bulk composition.

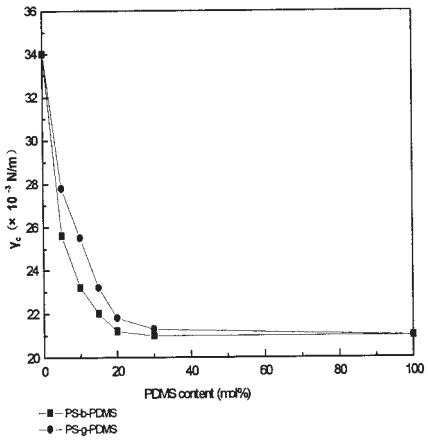

Figure 4 The surface energy of PS-PDMS copolymers.

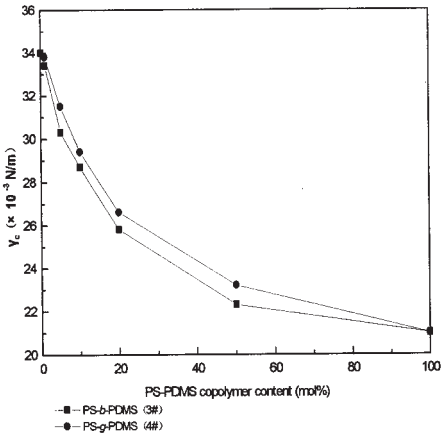

Figure 5. The surface energy of the PS-PDMS copolymers and the PS blend.

The surface tension of PS-PDMS copolymer and the copolymer and PS blend

Figure 4 shows that the surface tension of solvent-cast PS-PDMS diblock and graft copolymer films, at the air surface, dramatically decreased upon increasing the PDMS bulk content of PS-PDMS copolymers. However, beyond a "critical concentration" of 20 wt % of diblock copolymer, the surface tension of PS-PDMS copolymer films tended to level-off at a value, which was very close to the surface tension of PDMS. The experimental data reflected the significant immiscibility of PDMS and PS, and the strong propensity of PDMS to accumulate at the air surface uniformly. Meanwhile, a similar behavior was observed for the PS-PDMS graft copolymer at the air surface. However, as discussed previously, the PDMS segments in the block copolymers were much easier to accumulate at the surface than those in the graft copolymers. Consequently, the surface tension of the block copolymer was lower than that of the corresponding graft copolymer. Figure 5 shows the surface tension of PS-PDMS copolymer/PS blends at the air surface, as a function of PS-PDMS copolymer contents. As can be seen, the surface tension of PS films at the air surface decreased considerably upon the addition of increasing amounts of PS-PDMS copolymers. The surface tension of PS-*b*-PDMS/PS homopolymer blends was lower than that of the corresponding PS-*g*-PDMS/PS homopolymer blends. This phenomenon is attributed to the same reason as explained earlier.

CONCLUSIONS

The conclusions from this work are as follows:

- The enrichment of PDMS segments occurred on the surface of the block copolymers as well as on that of graft copolymers.

- The magnitude order of enrichment was as follows: PS-*b*-PDMS > PS-*g*-PDMS, due to the movement of the PDMS segments of PS-*b*-PDMS being facilitated.
- The PDMS segments migrated to the interface selectively; the accumulation of PDMS on the interface was also influenced by different solvents and substrates.
- The difference between the copolymers and solvents in solubility parameters also promoted the enrichment of PDMS segments on the surfaces.
- The PDMS distribution profiles further confirmed that the diblock copolymers tended to have higher surface segregation of the PDMS segments than that of the graft copolymers. This was also reflected in surface tension measurement.

References

1. Chen, X.; Gardella, J. A., Jr.; Kumler, P. L. Macromolecules 1992, 25, 6621.
2. Saam, J. C.; Gordon, D. J.; Lindsey, S. Macromolecules 1970, 3, 1.
3. Chen, X.; Gardella, J. A., Jr.; Kumler, P. L. Macromolecules 1992, 25, 6631.
4. Tezuka, Y.; Nobe, S.; Shimi, T. Macromolecules 1995, 28, 8251.
5. Petitjean, S.; Ghitti, G.; Jérôme, R.; Teyssié, P. Macromolecules 1994, 27, 4127.
6. Zhenguo, Z. Chem Res Appl 2000, 12, 370.
7. Yamashita, Y. J Macromol Sci Chem 1979, 13, 401.
8. Yamashita, Y.; Tsukahara, Y.; Ito, K.; Okada, K.; Tajima, Y. Polym Bull 1981, 5, 335.
9. Clark, D.; Peeling, J.; O'Malley, J. M. J Polym Sci Polym Chem Ed 1976, 14, 543.
10. Shuttleworth, D.; Van Dusen, J. G.; O'Malley, J. J.; Thomas, H. R. Polym Prepr (Am Chem Soc Div Polym Chem) 1979, 20, 499.
11. Duan, Y.; Pearce, E. M.; Kwei, T. K. Macromolecules 2001, 34, 6761.
12. Yang, X. M.; Peters, R. D.; Nealey, P. F. Macromolecules 2002, 35, 2406.
13. Budkowski, A.; Bernasik, A.; Cyganik, P.; Raczkowska, J.; Penc, B.; Bergues, B.; Kowalski, K.; Rysz, J.; Janik, J. Macromolecules 2003, 36, 4060.
14. Bes, L.; Huan, K.; Khoshdel, E.; Lowe, M. J.; McConville, C. F.; Haddleton, D. M. Eur Polym J 2003, 39, 5.
15. Petitjean, S.; Ghitti, G.; Fayt, R.; Jérôme, R.; Teyssié, P. Bull Soc Chim Belg 1990, 99, 997.
16. Xuelianbao, J. Theory and Practice of Anionic Polymerization; Chinese Fellowship Press: Beijing, 1990; p 237.
17. Hu, F.; Zheng, A.; Zhang, Q. The Surface and Interface of Polymer and Composite Material; China Light Industry Press: Beijing, 2001; p 55.